Available at WWW.MATHEMATICSWEB.ORG POWERED BY SCIENCE DIRECT®

Applied Mathematical Modelling 27 (2003) 491–513

APPLIED MATHEMATICAL MODELLING

www.elsevier.com/locate/apm

Approximate analytical model for solidification in a finite PCM storage with internal fins

Piia Lamberg *, Kai Sirén *

Helsinki University of Technology, HVAC Laboratory, P.O. Box 4400, 02015 Hut, Finland

Received 13 August 2002; received in revised form 10 February 2003; accepted 28 March 2003

Abstract

In latent heat storage internal heat transfer enhancement techniques such as fins have to be used because of the low heat conductivity of the phase change material. Internal heat transfer enhancement is essential, especially in a solidification process where the main heat transfer mode is conduction. The aim of this paper is to present a simplified analytical model which predicts the solid–liquid interface location and temperature distribution of the fin in the solidification process with a constant end-wall temperature in the finned two-dimensional PCM storage. The analytical results are compared to numerical results and they show that the analytical model is more suited to the prediction of the solid–liquid interface location than the temperature distribution of the fin in the PCM storage. A new factor called the fraction of solidified PCM is also introduced. The fraction of solidified PCM easily gives a good picture of how much of the storage is solidified after a given time.

Keywords: PCM; Heat transfer; Analytical model; FEMLAB

1. Introduction

Energy storage is essential whenever the supply or consumption of energy varies independently with time. Basically, there are three methods of storing thermal energy: sensible, latent and thermochemical heat or cold storage. Thermochemical storage offers an order of magnitude larger heat storage capacity compared to sensible heat storage. However, this technology is still in the development phase. A latent heat storage system (LHTS) is preferable to sensible heat storage in

* Corresponding authors. Tel.: +358-9-451-3597; fax: +358-9-451-3418 (P. Lamberg), Tel.: +358-9-451-3602; fax: +358-9-451-3418 (K. Sirén).

E-mail addresses: piia.lamberg@hut.fi (P. Lamberg), kai.siren@hut.fi (K. Sirén).

0307-904X/03/$ - see front matter
doi:10.1016/S0307-904X(03)00080-5

Nomenclature

c_p heat capacity, $J\,kg^{-1}\,K^{-1}$
D half thickness of the fin, m
E energy storage capacity, J
E' energy storage per unit length, $W\,m^{-1}$
E'' energy storage per unit area, $W\,m^{-2}$
f_i local solid fraction, –
H total enthalpy, J
h enthalpy, J
k heat conductivity, $W\,m^{-1}\,K^{-1}$
l length, m
L latent heat of fusion, $J\,kg^{-1}$
q heat flow, W
q' heat flow per unit length, $W\,m^{-1}$
q'' heat flux, $W\,m^{-2}$
S location of the phase change interface, m
St Stefan number, $St = (c_p\Delta T)/L$
T temperature, °C
ΔT_m solidification temperature range, °C
t time, s
x distance in the x-direction, m
y distance in the y-direction, m
Δx space increment in the x-direction
Δy space increment in the y-direction

Greek symbols
α thermal diffusivity, $m^2\,s^{-1}$
ρ density, $kg\,m^{-3}$
ε rate of solidified PCM
λ root of the transcendental equation
$\theta = \frac{T-T_m}{T_w-T_m}$ dimensionless temperature distribution
$\tau = \frac{k_f t}{(\rho c_p)_f l_f^2}$ dimensionless time
$\gamma = \frac{S_y}{l_c}$ dimensionless rate of solid–liquid interface recession
$\eta = \frac{x}{l_f}$ dimensionless x-coordinate
$\lambda = \frac{l_f}{l_c}$ cell aspect ratio
$\Psi = \frac{D}{l_c}$ dimensionless half thickness of the fin
$\kappa = \frac{k_s}{k_f}$ ratio of the heat conductivities
$\xi = \frac{(\rho c_p)_f (T_w-T_m)}{-L\rho_s}$ modified Stefan number

Subscripts and superscripts

c	convection
d	depth
f	fin
l	liquid
m	solidification
old	old value
p	phase change material
s	solid
t	theoretical
w	wall
x	*x*-direction
y	*y*-direction
2D	two-dimensional

applications with a small temperature swing because of its nearly isothermal storing mechanism and high storage density.

A common problem in latent heat thermal storages is the poor conductivity of the phase change materials. The crystallising and thickening agents which prevent supercooling and phase separation in the PCM lower the thermal conductivity of the PCM and the inhibiting convection motion in the liquid PCM [1,2]. During the phase change the solid–liquid interface moves away from the heat transfer surface. Thus, the surface heat flux decreases due to the increasing thermal resistance of the growing layer of molten or solidified PCM. The problem arises especially in solidification processes where the sole heat transfer mode is conduction.

PCM melts more quickly than it solidifies because natural convection speeds up the melting of PCM. In solidification the heat transfers by conduction in solid PCM out from the storage. If there is a temperature gradient in liquid PCM, natural convection exists in the liquid–solid interface. But even very strong natural convection has a negligible effect on the solid–liquid interface position compared to the effect of heat conduction in solid PCM [3,11]. PCM solidifies on the heat transfer surface and acts as a self-insulator because of low heat conductivity. In practice some kind of heat transfer enhancement technique has to be used in LHTS because of the low heat conductivity of the PCM. Heat transfer in LTHS can be enhanced by the following techniques:

(a) Active methods such as agitators/vibrators, scrapers and slurries [4].
(b) Using microencapsulated PCM [5].
(c) Using PCM containing dispersed high conductivity particles or lessing rings [6].
(d) Using PCM graphite composite material [7].
(e) Using extended surfaces such as fins and honeycombs [1,2,11,12].

This paper focuses on the finned PCM storage and heat transfer enhancement in the solidification process. Heat transfer during solidification in a storage with internal fins has been studied

numerically and experimentally by many authors. Velraj et al. [8] made an experimental analysis and numerical modelling of inward solidification on a finned vertical tube for a latent heat storage unit. The solidification time in a finned tube was reduced approximately by a factor $1/n$ (where n is the number of fins in the tube) compared to the case without fins. Velraj et al. [2] also studied experimentally and numerically different heat transfer enhancement techniques for a solar thermal storage system focusing on fins, lessing rings and air bubbles.

Al-Jandal [9] studied experimentally what effects the fin, metal honeycomb and copper matrix structure have on the total melting and solidification time. The results showed that the average thermal conductivity enhancement factors for solidification are in the order of 1.7 and those for melting in the order of 3.3. Natural convection has a significant effect on the acceleration of melting. The average thermal conductivity enhancement factor was determined as a ratio of solidification or melting time with fins and without fins.

Bugaje [10] conducted experiments on the use of methods for enhancing the thermal response of paraffin wax heat storage tubes by the incorporation of aluminium fins and star structures. The conclusion was that internal fins performed much better than the star matrices, reducing the loading time in the order of 2.2 and the unloading time in the order of 4.2.

Padmanabhan and Murthy [1] presented a theoretical analysis for phase change in a cylindrical annulus with axial rectangular fins between inner and outer tubes. The finite-difference method was used. Based on the analysis, a working formula for the volume of the melt/frozen fraction for PCM was introduced for engineering purposes. The analysis also indicated that the addition of fins in the cylindrical annulus is advantageous for energy storage applications. The melting or solidification time decreases with an increase in the number of fins. The fins should be long and thin and they should be made of good thermal conductors.

Stritih and Novak [11] handled numerically and experimentally heat transfer enhancement in the solidification process in a finned PCM storage with a heat exchanger. The conclusion arrived at was that the biggest influence on heat transfer in the solidification process was the distance between the fins. The thickness of the fin is not as influential.

Humphries and Griggs [12] studied numerically a rectangular phase change housing, using straight fins as a heat transfer enhancer in a two-dimensional grid. The data were generated over a range of realistic sizes, material properties and different kinds of thermal boundary conditions. This resulted in a design handbook for phase change energy storage.

It is obvious that fins enhance the internal heat transfer of a phase change storage. Fins have a larger influence on the solidification process than on the melting process. If fins are near each other, the effect of natural convection decreases when conduction takes place as the prime heat transfer mode in a melting process. Melting slows down while solidification speeds up when the fins enhance conduction heat transfer in the storage. The loading and unloading times have to be optimised to achieve the best technical performance for the storage. Here the geometry of the latent heat storage plays a very important role.

Heat transfer in finned PCM storages has been widely studied but analytical models for the solidification process have not been published. The main advantages of an analytical model are simplicity and short computation times. These features can be valuable in certain situations, such as in the pre-design stage of the storage. Absolute precision is not important in such a situation but the speed of the calculation is, as it enables us to compare several alternatives within a reasonable time.

Lamberg et al. have derived an analytical model for the melting process in a finned semi-infinite storage [13]. This paper continues work already carried out on the solidification process. The objective of this work was to develop an approximate analytical model for the solidification process in a finite PCM storage with internal fins.

2. Finite PCM storage with internal fins

In this work the solidification process in a finite two-dimensional PCM storage with internal fins is studied (Fig. 1). Basically, the PCM storage consists of a metallic housing in the shape of a parallelepiped which is filled with PCM and straight metal fins. These improve heat transfer between the housing and the PCM.

Initially the PCM is in a liquid phase in the storage. During solidification the PCM storage operates as a heat source when the right and left end-walls are kept at a constant temperature, one which is lower than the initial temperature of the liquid PCM ($T_w < T_i$). The phase change material releases energy primarily via the phase change process. Heat transfers by conduction along the fins and through the solidified phase change material from the solid–liquid interface to the end-walls.

This problem is a so called Stefan-type problem or a moving boundary problem, whose basic feature is that the regions in which the partial differential equations are held are unknown and must be found as part of the solution to the problem. This amounts to a non-linearity of geometric nature even when the rest of the equations appear to be linear. Non-linearity is the source of difficulties in moving boundary problems. The non-linearity destroys the validity of generally used solving methods such as the superposition method and the separation of variables method [15]. The analytical solution to this kind of two-dimensional heat transfer problem with a phase change has not been found. However, the problem is sufficiently simple to be solved numerically by using well-known numerical methods such as the enthalpy method or the effective heat capacity method, along with the finite difference or finite element procedure.

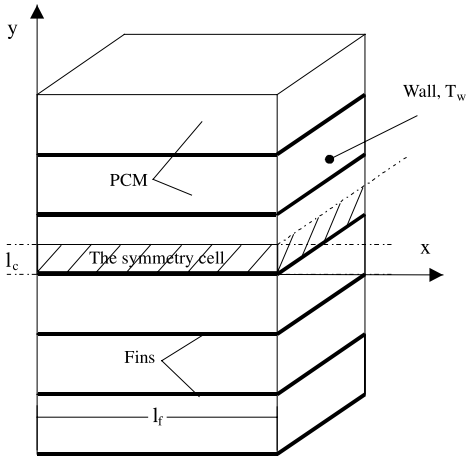

Fig. 1. A finite PCM storage with internal fins.

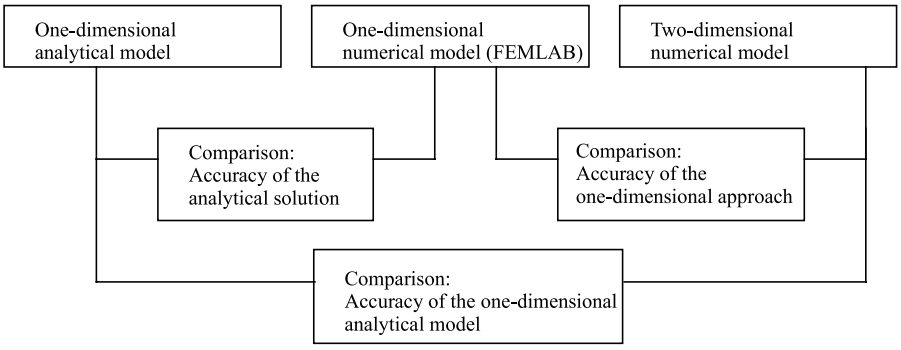

Fig. 2. Methodology to find out the effect of different simplifications.

In this paper a simplified one-dimensional analytical model based on a quasi-linear, transient, thin-fin equation is presented. The model predicts the solid–liquid interface location and the temperature distribution of the fins during the solidification process in the storage. A new factor called the fraction of solidified PCM may be calculated from the results of the analytical solution.

In addition to the one-dimensional analytical model, the heat transfer in the PCM storage is calculated with a simplified one-dimensional numerical model and a two-dimensional numerical model. The one-dimensional numerical calculation is carried out using a programme known as FEMLAB, which is a simulation package solving systems and coupled equations through the finite element method in one-, two- and three-dimensions [14]. The two-dimensional numerical calculation is based on the enthalpy method and implemented in the Digital Fortran 5.0 environment. By comparing the results of different methods it is possible to draw conclusions about the accuracy of the one-dimensional analytical model (Fig. 2).

3. One-dimensional approach

The heat transfer in a PCM storage with internal fins cannot be solved analytically in a two-dimensional case. In this paper a simplified one-dimensional model is introduced to determine analytically the temperature of the fin and the location of the solid–liquid interface during the solidification.

The PCM storage has a symmetrical structure. Therefore, the analysis is reduced to handle only a one symmetry cell where the planes of symmetry are in the middle of the fin and midway between the two adjacent fins (Fig. 3). The symmetry cell is divided into two regions. In region 1, the only heat sink is the constant temperature end-wall. Here the fin does not influence the solidification process. In region 2, both the wall and the fin transfer heat from the phase change material to the environment.

3.1. Assumptions

Due to the non-linear, unsteady nature of the problem several assumptions have been made to simplify the two-dimensional heat transfer problem.

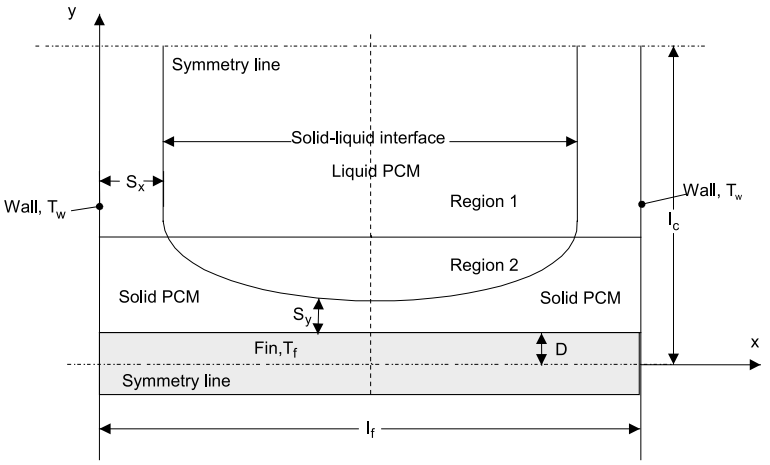

Fig. 3. The symmetry cell of PCM storage with an internal fin.

1. Initially the liquid PCM and the fin are at the solidification temperature of the phase change material $T_m = T_l = T_f$. Therefore, the heat conduction and natural convection in the liquid PCM are considered to be negligible. The sole heat transfer is by conduction in the solid PCM.
2. The solidification temperature (T_m) is assumed to be constant. In reality, a phase change material has a solidification range (ΔT_m).
3. The temperature distribution of the fin is considered to be one-dimensional in the x-direction because the fin is thin and the conductivity of the fin material is high.
4. In region 1, heat transfer is one-dimensional only in the x-direction. The fin does not affect heat transfer in this region.
5. In region 2, the solid–liquid interface moves only one-dimensionally in the y-direction because the heat is mainly transferred through the fin to the environment.
6. In region 2, the sensible heat of solid PCM is assumed to be negligible. The latent heat of fusion is assumed to be the principal mode of energy storage. In region 1, the sensible heat is taken into account.
7. The physical properties such as heat conductivity, heat capacity and density of the phase change material and the fin are assumed to be constant.

3.2. Mathematical formulation

Following the previously introduced regions the mathematical formulation will also be divided into two parts. In region 1 the solidification can be handled as a one-dimensional one-phase Stefan problem [15], which is the simplest explicitly solvable moving boundary problem with constant end-wall temperature and with constant thermophysical properties in the materials. In a one-phase Stefan problem the heat equation for a solid phase change material and for a solid–liquid interface with an initial and boundary conditions is:

$$\frac{\partial^2 T_s}{\partial x^2} = \frac{1}{\alpha_s}\frac{\partial T_s}{\partial t}, \quad t > 0, \;\; 0 \leqslant x \leqslant l_f \tag{1}$$

$$-(\rho L)_{\mathrm{s}}\frac{\partial S_x(t)}{\partial t} = -k_{\mathrm{s}}\frac{\partial T_{\mathrm{s}}(S_x,t)}{\partial x}, \quad t>0 \tag{2}$$

$$S_x(0) = 0 \tag{3}$$

$$T_{\mathrm{s}}(S_x,t) = T_{\mathrm{m}} \tag{4}$$

$$T_{\mathrm{s}}(0,t) = T_{\mathrm{s}}(l_{\mathrm{f},},t) = T_{\mathrm{w}} \tag{5}$$

In region 2 the movement of solid–liquid interface is assumed to occur only in the y-direction. An arbitrary differential element, dx, is separated from the PCM storage to outline energy balances in Fig. 4. The energy balance of the element dx yields two equations, one for the fin and one for the PCM.

The energy balance for the fin is

$$E''_{\mathrm{f}} = -q''_x + q''_{x+\mathrm{d}x} - q''_{\mathrm{c}} \tag{6}$$

The rate equations are substituted into the energy balance Eq. (6) which can be rewritten with initial and boundary conditions as

$$(\rho c_p)_{\mathrm{f}} D\frac{\partial T_{\mathrm{f}}}{\partial t} = k_{\mathrm{f}} D\frac{\partial^2 T_{\mathrm{f}}}{\partial x^2} - \frac{k_{\mathrm{s}}}{S_y}(T_{\mathrm{f}} - T_{\mathrm{m}}), \quad t>0 \tag{7}$$

$$T_{\mathrm{f}}(x,0) = T_{\mathrm{m}} \tag{8}$$

$$T_{\mathrm{f}}(0,t) = T_{\mathrm{w}} \tag{9}$$

$$T_{\mathrm{f}}(l_{\mathrm{f}},t) = T_{\mathrm{w}} \tag{10}$$

The energy balance for the solid–liquid interface recession in the y-direction is

$$E'_{\mathrm{p}} = q'_{\mathrm{w}} + q'_{\mathrm{c}} \tag{11}$$

The released heat due to solidification in a dx wide element is

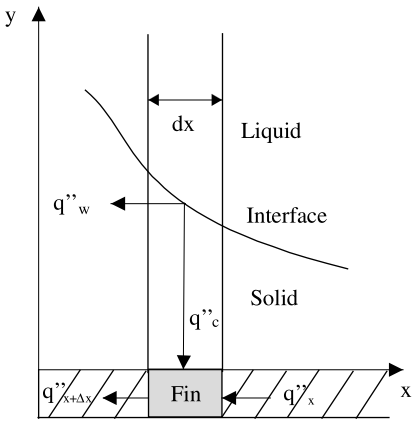

Fig. 4. Energy flows in a differential element in the finned PCM storage.

$$E'_{\mathrm{p}} = -(\rho L)_{\mathrm{s}} \frac{\partial S_y}{\partial t}\,\mathrm{d}x \tag{12}$$

The heat transfer from the solid–liquid interface to the fin takes place by conduction and is

$$q'_{\mathrm{c}} = \frac{k_{\mathrm{s}}}{S_y}(T_{\mathrm{f}} - T_{\mathrm{m}})\,\mathrm{d}x \tag{13}$$

The rate of heat flow per unit length from the solid–liquid interface to the constant temperature end-walls q_{w} is determined by conduction through the solid in the x-direction:

$$q'_{\mathrm{w}} = \frac{k_{\mathrm{s}}}{x}(T_{\mathrm{w}} - T_{\mathrm{m}})\frac{\partial S_y}{\partial x}\,\mathrm{d}x \tag{14}$$

After substituting Eqs. (12)–(14) into the energy balance Eq. (11) it can be rewritten with the initial condition as

$$-(\rho L)_{\mathrm{s}} \frac{\partial S_y}{\partial t} = \frac{k_{\mathrm{s}}}{x}(T_{\mathrm{w}} - T_{\mathrm{m}})\frac{\partial S_y}{\partial x} + \frac{k_{\mathrm{s}}}{S_y}(T_{\mathrm{f}} - T_{\mathrm{m}}), \quad t > 0 \tag{15}$$

$$S_y(x, 0) = 0 \tag{16}$$

To enable a simpler manipulation, Eqs. (7)–(10), (15) and (16) are converted into dimensionless form. The following dimensionless variables are introduced [16]:

$\theta = \dfrac{T - T_{\mathrm{m}}}{T_{\mathrm{w}} - T_{\mathrm{m}}}$, dimensionless temperature distribution

$\tau = \dfrac{k_{\mathrm{f}} t}{(\rho c_p)_{\mathrm{f}} l_{\mathrm{f}}^2}$, dimensionless time

$\gamma = \dfrac{S_y}{l_{\mathrm{c}}}$, dimensionless rate of solid–liquid interface recession

$\eta = \dfrac{x}{l_{\mathrm{f}}}$, dimensionless x-coordinate

$\lambda = \dfrac{l_{\mathrm{f}}}{l_{\mathrm{c}}}$, cell aspect ratio

$\Psi = \dfrac{D}{l_{\mathrm{c}}}$, dimensionless half thickness of the fin

$\kappa = \dfrac{k_{\mathrm{s}}}{k_{\mathrm{f}}}$, ratio of the heat conductivities

$\xi = \dfrac{(\rho c_p)_{\mathrm{f}}(T_{\mathrm{w}} - T_{\mathrm{m}})}{-L\rho_{\mathrm{s}}}$, modified Stefan number

Eqs. (7)–(10), rewritten using the dimensionless variables determine the dimensionless temperature distribution as a function of dimensionless time and length along the finite fin with the initial and boundary conditions:

$$\frac{\partial\theta}{\partial\tau} = \frac{\partial^2\theta}{\partial\eta^2} - \frac{\lambda^2\kappa}{\Psi}\frac{\theta}{\gamma}, \quad \tau > 0 \tag{17}$$

$$\theta(\eta, 0) = 0 \tag{18}$$

$$\theta(0, \tau) = 1 \tag{19}$$

$$\theta(1, \tau) = 1 \tag{20}$$

Eqs. (15) and (16), rewritten in dimensionless form, determine the dimensionless rate of solid–liquid interface recession as a function of dimensionless place along the fin:

$$\frac{\partial\gamma}{\partial\tau} = \frac{\xi\kappa}{\eta}\frac{\partial\gamma}{\partial\eta} + \xi\kappa\lambda^2\frac{\theta}{\gamma}, \quad \tau > 0 \tag{21}$$

$$\gamma(\eta, 0) = 0 \tag{22}$$

Eqs. (17)–(22) form the basis for the simplified one-dimensional model.

3.3. Analytical solution of the simplified one-dimensional model

In region 1 the Stefan problem Eqs. (1)–(5) has a well-known analytical solution. According to Neumann [15], the distance of the solid–liquid interface from the left end wall can be solved from Eqs. (23) and (24):

$$S_{x=0} = 2\lambda\sqrt{\alpha_s t} \tag{23}$$

where λ is a root of the transcendental equation

$$\lambda e^{\lambda^2}\mathrm{erf}(\lambda) = \frac{St_l}{\sqrt{\pi}} = \frac{c_p(T_w - T_m)}{-L\sqrt{\pi}} \tag{24}$$

Due to the symmetry, the distance of the solid–liquid interface from the right end wall is

$$S_{x=L_f} = l_f - S_{x=0} \tag{25}$$

In region 2, for the dimensionless equations (17)–(20) no mathematically exact solution exists. Eq. (17) is a parabolic partial differential equation and it is impossible to solve with known methods because the dimensionless rate of the solid–liquid interface recession γ is a variable in the equation. Eq. (21) shows that γ is a function of the dimensionless place η and time τ. The following assumptions are made to make the dimensionless equations solvable:

1. The dimensionless rate of the solid–liquid interface recession γ is assumed to be constant in Eq. (17). By introducing a new parameter $v = (\lambda^2\kappa)/(\Psi\gamma)$, Eq. (17) it can be rewritten as

$$\frac{\partial\theta}{\partial\tau} = \frac{\partial^2\theta}{\partial\eta^2} - v\theta, \quad \tau > 0 \tag{26}$$

2. The dimensionless temperature distribution θ is assumed to be constant in Eq. (21) and the dimensionless rate of the solid–liquid interface recession γ is assumed to be only the function of dimensionless time. Hence, Eq. (21) can be rewritten as

$$\frac{\partial\gamma}{\partial\tau} = \xi\kappa\lambda^2\frac{\theta}{\gamma}, \quad \tau > 0 \tag{27}$$

First, the dimensionless temperature distribution of the fin is solved from Eq. (26) and (18)–(20). Eq. (26) is a parabolic partial differential equation and its solution is well-known with given initial and boundary conditions [17]:

$$\theta = \frac{\cosh((\eta - 0.5)\sqrt{v})}{\cosh(0.5\sqrt{v})} - \frac{4}{\pi e^{v\tau}}\sum_{n=0}^{\infty}\frac{(-1)^n e^{(-(2n+1)^2\pi^2\tau)}}{(2n+1)[1 + \{v/((2n+1)^2\pi^2)\}]}\cos((2n+1)\pi(\eta - 0.5)) \tag{28}$$

The dimensionless rate of the solid–liquid interface recession γ is solved from the Eqs. (27) and (22) to give

$$\gamma = \sqrt{2\xi\kappa\lambda^2\theta\tau} \tag{29}$$

Eqs. (28) and (29) are solved and the solution for the dimensionless temperature distribution of the fin and the dimensionless rate of the solid–liquid interface recession are found. Finally, the temperature distribution of the fin and the distance of the solid–liquid interface in the y-direction are

$$T = T_m + \theta(T_w - T_m) \tag{30}$$

and

$$S_y = l_c\gamma \tag{31}$$

In conclusion, the analytical solution for the simplified one-dimensional heat transfer problem consists of the Neumann solution for the solid–liquid interface location S_x in the x-direction in region 1 (Eqs. (23)–(25)) and of the derived analytical solution for the temperature distribution of the fin T_f and the solid–liquid interface location S_y in y-direction in region 2 (Eqs. (28)–(31)).

3.4. Numerical solution

Eqs. (7)–(10), (15) and (16) are solved numerically with the FEMLAB programme [14]. FEMLAB is based on the finite element method and is a powerful tool for solving coupled systems of non-linear partial differential equations in one-, two- or three-dimensions. The geometry of the storage is defined. The equations are written in partial differential form in line with programme definitions, and initial and boundary conditions are determined. The numerical solution achieved is compared to the analytical solution to find out how the assumptions made influence the simplified solution.

4. Two-dimensional approach

To determine the accuracy of the one-dimensional approach and the analytical model, a two-dimensional numerical model is also developed and implemented. Here, the numerical analysis is also reduced to only handle a one symmetry cell where the planes of symmetry are located in the middle of the fin and midway between two adjacent fins (Fig. 2).

4.1. Assumptions

Assumptions 1, 2 and 7 made in Section 3.1 are also valid for the two-dimensional model. The heat transfer is two-dimensional in the storage and the sensible heat of PCM is taken into account. The whole storage is initially in its solidification temperature. Thus, there is no temperature gradient in the liquid and natural convection is negligible and it can thus be ignored.

4.2. Mathematical formulation

The following two-dimensional heat equation can be applied for the fin and for the phase change material:

$$\left(\frac{\partial^2 T}{\partial x^2}+\frac{\partial^2 T}{\partial y^2}\right)=\frac{1}{\alpha}\frac{\partial T}{\partial t}, \quad t>0 \tag{32}$$

$$T(x,y,0)=T_{\mathrm{m}} \tag{33}$$

$$T(0,y,t)=T(l_{\mathrm{f}},y,t)=T_{\mathrm{w}} \tag{34}$$

where T is the temperature of the fin or PCM, α is the thermal diffusivity of the fin or PCM respectively.

The two-dimensional heat equation for the solid–liquid interface location is [18]:

$$k_{\mathrm{s}}\left(\frac{\partial T_{\mathrm{s}}}{\partial y}\right)\left[1+\left(\frac{\partial S_y}{\partial x}\right)^2\right]=\rho_{\mathrm{s}} L\frac{\partial S_y}{\partial t}, \quad y=S_y \tag{35}$$

The two-dimensional model with initial and boundary conditions can be solved numerically, but it is not possible to find an analytical solution for this kind of heat transfer problem with a phase change.

4.3. Numerical solution

The enthalpy method with a finite volume procedure is used to simulate the temperature distribution and the solid–liquid interface location in the storage [4,15]. The enthalpy method is used in a particular way so that the only unknown variable is the temperature of the phase change material and the solidification occurs at a uniform temperature. A Fortran code was developed to carry out the calculations.

Zivkovic and Fujii [19] have used this method in a one-dimensional PCM storage. In this paper the method is conducted, presented and used in a two-dimensional form. The enthalpy equation for the conduction-controlled heat transfer in PCM and the fin can be written as

$$\frac{\partial H}{\partial t} = \frac{k}{\rho}\left(\frac{\partial^2 T}{\partial x^2} + \frac{\partial^2 T}{\partial y^2}\right) \tag{36}$$

where H is the total enthalpy. An alternative form for Eq. (36) can be written by splitting the total enthalpy into sensible and latent heat components:

$$H = h + Lf_i \tag{37}$$

where h is sensible enthalpy and f_i the local solid fraction. The sensible heat component can further be written as

$$h = \int_{T_m}^{T} c_p \, \mathrm{d}T \tag{38}$$

where c_p is the heat capacity of the material. For an isothermal phase change the local solid fraction f_i in the solidification process is defined as:

$$f_i(T) = \begin{cases} 0-1 & \text{if } T = T_m \\ 1 & \text{if } T < T_m \\ 0 & \text{if } T > T_m \end{cases} \tag{39}$$

Substituting Eq. (37) into Eq. (36) gives the following with initial and boundary conditions:

$$\frac{\partial h}{\partial t} = \frac{k}{\rho}\left(\frac{\partial^2 T}{\partial x^2} + \frac{\partial^2 T}{\partial y^2}\right) - L\frac{\partial f_i}{\partial t}, \quad t > 0 \tag{40}$$

$$T_f(x, y, 0) = T_s(x, y, 0) = T_m \tag{41}$$

$$T_f(0, y, t) = T_s(0, y, t) = T_f(l_f, y, t) = T_s(l_f, y, t) = T_w \tag{42}$$

$$T_f(x, D, t) = T_s(x, D, t) \tag{43}$$

In cases where solidification occurs in the node (i, j), the solid fraction lies in the interval [0,1] and $\partial h/\partial t = 0$. Eq. (40) is fully implicit discretized in each internal node (i, j) and it can be written as

$$f_{i,j} = f_{i,j}^{\text{old}} + \frac{k_i \Delta t}{\rho_i L \Delta x^2}(T_{i-1,j} - 2T_{i,j} + T_{i+1,j}) + \frac{k_i \Delta t}{\rho_i L \Delta y^2}(T_{i,j-1} - 2T_{i,j} + T_{i,j+1}) \tag{44}$$

where Δx is the space increment in the x-direction and Δy is the space increment in the y-direction. Eq. (44) updates the solid fraction during the phase change process.

In cases where the PCM is fully solid or liquid, Eq. (40) reduces to the ordinary heat diffusion equation and its discretized form is

$$T_{i,j} = T_{i,j}^{\text{old}} + \frac{k_i \Delta t}{\rho_i c_{pi} \Delta x^2}(T_{i-1,j} - 2T_{i,j} + T_{i+1,j}) + \frac{k_i \Delta t}{\rho_i c_{pi} \Delta y^2}(T_{i,j-1} - 2T_{i,j} + T_{i,j+1}) \tag{45}$$

At the end of each time step, the check for the start and/or end of the phase change has to be performed throughout the entire domain. If solidification begins or ends during the calculated time step, the calculation has to be performed again. When the solidification begins, the sensible heat released to lower the temperature of the control volume to the solidification temperature can not be used for solidification in the PCM, and when solidification ends the heat released to complete solidification cannot be used either to lower the temperature of the PCM.

A Visual Fortran 5.0 code was developed to solve Eqs. (41)–(45) with different time steps. In the simulation model the storage consists of a two-dimensional fixed grid. The space increments depend on the dimensions of the storage.

After each time step each node gets a new value for the temperature and for the solid fraction. The location of the solid–liquid interface is interpolated between the nodes.

The model was tested by comparing the released energy from the storage during a specified calculation period to the theoretical storage capacity. The theoretical capacity E'_t of the storage with a temperature difference $T_1 - T_2$ is

$$E'_t = m_\mathrm{p} c_p (T_1 - T_2) + m_\mathrm{f} c_{p\mathrm{f}} (T_1 - T_2) + m_\mathrm{p} h_\mathrm{f} \tag{46}$$

where m_p is the mass of the PCM and m_f the mass of the fin. This was compared with the released energy $E'_{2\mathrm{D}}$ from the storage during the two-dimensional numerical calculations

$$E'_{2\mathrm{D}} = \Delta y \sum_{k=1}^{m} \sum_{j=1}^{n} \frac{k_j \Delta T_{k,j}}{\Delta x} \Delta t_k \tag{47}$$

$$\sum_{k=1}^{m} \Delta t_k = t, \quad j = 1, 2, \ldots, n \text{ and } k = 1, 2, \ldots, m$$

where t is the total calculation time and $\Delta T_{k,j}$ the temperature difference in node j in time k.

The error produced was smaller than 0.1% when the theoretical storage capacity and the released energy during the two-dimensional calculation were compared with each other. Zivkovic and Fujii [19] examined the accuracy of the method in a one-dimensional case. They obtained only 0.12% error in the location of the solid–liquid interface in one-dimensional calculations when compared to the enthalpy based approach where the enthalpy is a function of the temperature.

5. Results

5.1. Test cases

To find out the accuracy and performance of the one-dimensional approach and the analytical solution, six different test cases were chosen. In the test cases laboratory grade pure *n*-octadecane paraffin with an aluminium fin (three cases) and a commercial grade salt hydrate (Climsel 23) with a steel fin (three cases) were chosen. *n*-Octadecane paraffin has a relatively uniform melting point, but the salt hydrate melts and solidifies in temperature range 21–25 °C [16,20]. However, it has been assumed that the both PCMs have a discrete melting temperature, though in reality they have a melting region. The melting temperature of the salt hydrate was fixed at 23 °C, which is the

Table 1
Physical properties of the phase change and the fin materials

Property	Paraffin *n*-octadecane	Salt hydrate Climsel 23	Aluminium fin	Steel fin
Density (ρ), kg m^{-3}	777	1480	2713	7854
Heat conductivity (k), W m^{-1} K^{-1}	0.149	0.6	180	60.5
Heat capacity (c_p), J kg^{-1} K^{-1}	2660	2660	960	434
Latent heat of fusion (L), J kg^{-1}	241,360	148,000	–	–
Melting/solidification temperature (T_m), °C	28	23	–	–

average temperature in the melting and solidification range of salt hydrates. The physical properties of the phase change and the fin materials are shown in Table 1 [16,21].

In the test cases the initial temperature of the storage is the solidification temperature and the PCM is in liquid state. The temperature difference ($T_m - T_w$) in all cases is fixed at 15 °C. The half thickness D of the fin has a constant value. Otherwise, the geometry of the storage is varied in different cases. The width to height ratio $\lambda = L_f/L_c$ varies between 0.2 and 5.

The geometry of the storage affects the speed of the solidification. When λ is small, the heat transfers mainly through the wall from the solid–liquid interface to the environment. When λ is close to one, the influence of the wall and the fin are of the same magnitude and when λ is large, the fin has a major role in heat transfer. Therefore, when λ is small, the speed of the solid–liquid interface in the x-direction determines the solidification time and when λ is large, the speed of the interface in the y-direction determines the solidification time. Three different λ values were used. The calculation time is also varied. The geometry, initial temperatures, materials and calculation times used in different test cases are shown in Table 2.

For each test case the location of the solid–liquid interface and the temperature of the fin are calculated using three different methods:

1. simplified one-dimensional analytical model,
2. simplified one-dimensional numerical model, and
3. two-dimensional numerical model.

Table 2
The geometry of the storage, initial temperatures, materials and calculation time used in different test cases

	Case 1	Case 2	Case 3	Case 4	Case 5	Case 6
PCM	Paraffin	Paraffin	Paraffin	Salt hydrate	Salt hydrate	Salt hydrate
Fin	Aluminium	Aluminium	Aluminium	Steel	Steel	Steel
Tm, °C	28	28	28	23	23	24
Tw, °C	13	13	13	8	8	8
Lf, m	0.01	0.05	0.05	0.01	0.05	0.05
Lc, m	0.05	0.05	0.01	0.05	0.05	0.01
$\lambda = L_f/L_c$	0.2	1	5	0.2	1	5
D, m	0.0005	0.0005	0.0005	0.0005	0.0005	0.0005
t, s	723	1085	1085	169	4226	1127
τ, –	500	30	30	30	30	6

The results achieved with different methods are compared with each other in line with the methodology shown in Fig. 2.

5.2. Accuracy of the one-dimensional approach

Several assumptions were made in the simplified one-dimensional model (see Section 3.1). By comparing the numerical results of the simplified one-dimensional model to the numerical results of the two-dimensional model it is possible to draw conclusions about the error made when using a one-dimensional model instead of a two-dimensional model.

The one-dimensional numerical results in region 2 are calculated using FEMLAB (Eqs. (7)–(10) and (15) and (16), and the two-dimensional numerical results using the enthalpy method (Eqs. (44)–(46)) with Visual Fortran 5.0 code. In region 1, the location of the solid–liquid interface has an exact analytical solution from Neumann. Therefore, the one-dimensional numerical solution in region 1 does not need to be calculated. The step size is $\Delta\eta = 0.1$ in the x-direction both in one- and two-dimensional numerical results. The step size does not affect the results. In Fig. 5a–f, the temperature distributions of the fin in different test cases are shown.

It seems that the accuracy of the one-dimensional numerical solution for the temperature distribution of the fin is good in cases where the width to height ratio (λ) is small. In this case the heat transfers mainly through the wall to the environment. The fin temperature approaches the wall temperatures quite quickly and the small amount of heat, which is transferred through the fin, is conducted effectively. The heat transfer is close to one-dimensional in the x-direction and, therefore, the one-dimensional model gives good results.

The biggest error is made when λ approaches value one. In this scenario, the temperature difference between one-dimensional and two-dimensional numerical results is 1–2 °C in both paraffin and salt hydrate storage. When λ is equal to one the wall has a strong effect on the solidification process, but in the simplified one-dimensional model it is assumed that the solid–liquid interface moves only in the y-direction when the temperature distribution of the fin is solved. It will distort the temperature distribution of the fin. In this case the storage should be handled two-dimensionally instead of one-dimensionally to achieve more accurate results.

When λ is large, the accuracy of a one-dimensional numerical solution for the temperature distribution of the fin is relatively good because the heat transfers mainly through the fin to the environment, as is assumed in the one-dimensional model.

In Fig. 6a–f, one- and two-dimensional numerical predictions of the solid–liquid interface location in the different test cases are shown.

When λ is small, the speed of the solid–liquid interface in the one-dimensional cases is slower than in the two-dimensional cases. It is possible to see from the figures that the cross-section of the one-dimensional results in region 1 and region 2 is sharp. It should be more round in the corners because of the two-dimensional heat transfer in that section. When λ increases, the location of the solid–liquid interface in the one-dimensional model will go ahead of the interface location in the two-dimensional model. This is due to the heat capacity of the PCM, which was ignored in region 2 in the one-dimensional approach. When λ is large, the fin plays the most important role in transferring heat out from the storage. In reality the heat capacity of the PCM slows down the speed of the solid–liquid interface in the solidification process. However, the error made in the

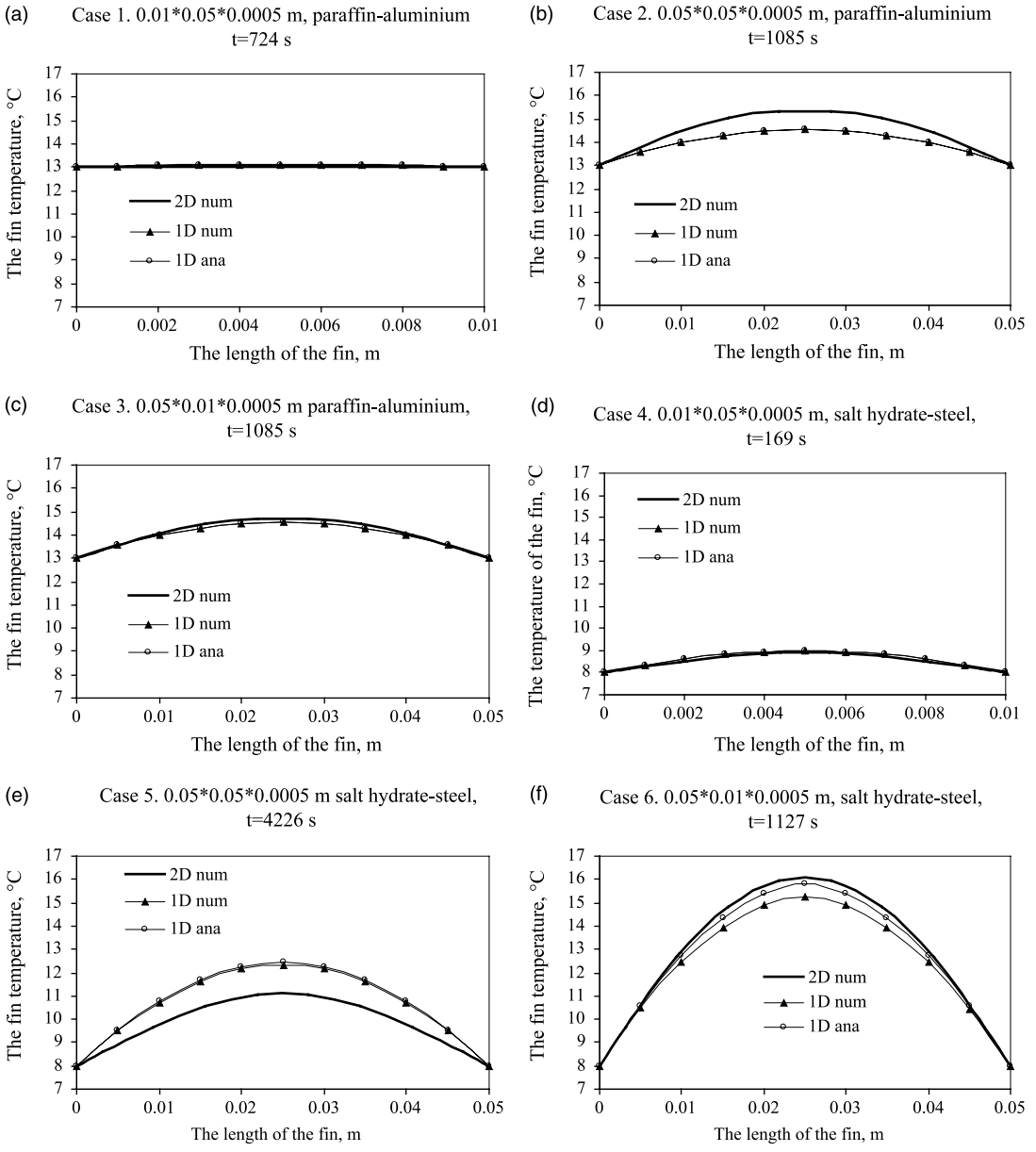

Fig. 5. (a–f) The one-dimensional analytical and numerical results and two-dimensional numerical results of the temperature distribution of the fin in different test cases.

solid–liquid interface location when using the one-dimensional model is not large in the calculated cases.

The one-dimensional model gives quite good results for the solid–liquid interface location but the results for the temperature distribution of the fin are not so good, except where λ is small. All

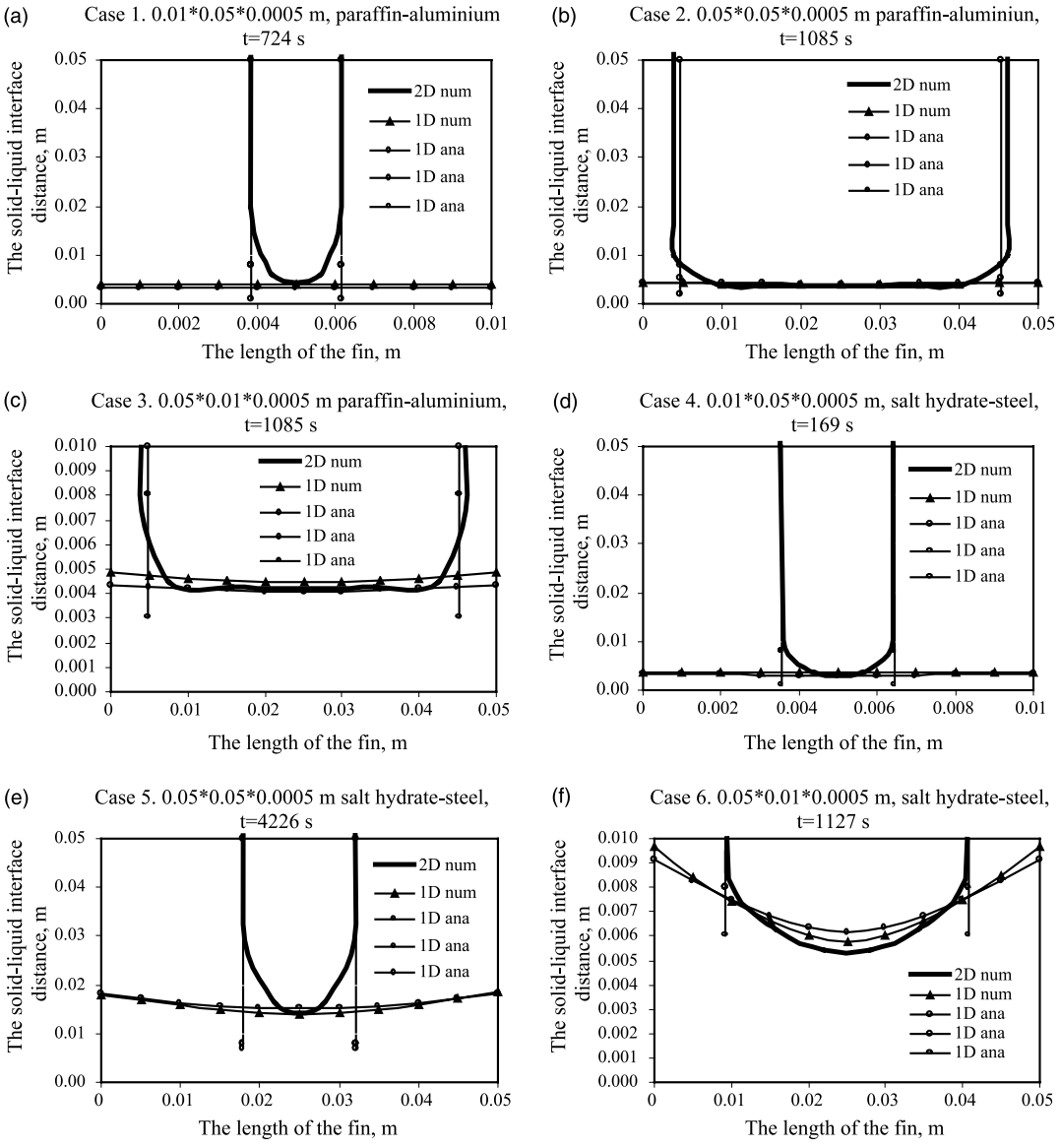

Fig. 6. (a–f) The one-dimensional analytical and numerical results and two-dimensional numerical.

in all, the one-dimensional model is better at predicting the solid–liquid interface location than the temperature distribution of the fin.

5.3. Accuracy of the analytical solution

The simplified one-dimensional model consists of a Neumann solution in region 1 and a derived analytical solution in region 2. Since the Neumann solution is an exact solution, there is no need

to study its accuracy. However, several assumptions are made when solving Eqs. (17)–(22) in region 2 to achieve the derived analytical solution for the location of solid–liquid interface in the y-direction and the temperature distribution of the fin.

By comparing the derived analytical solution to the one-dimensional numerical solution, with both having the same physical assumptions and mathematical formulation, it is possible to draw conclusions about the accuracy of the analytical solution.

The analytical results are calculated using Eqs. (23)–(25) and (28)–(31). The one-dimensional numerical calculation based on Eqs. (7)–(10), (15) and (16) is carried out using FEMLAB [14]. In Fig. 5a–f, the one-dimensional analytical and numerical results of the temperature distribution of the fin in different test cases are shown.

The maximum temperature difference (ΔT_{max}) between one-dimensional analytical and numerical results is small, especially in paraffin storage. The heat conductivity of the paraffin is poor whilst the heat conductivity of the aluminium fin is good. The temperature distribution of the fin approaches the temperature of the wall quite quickly. At the same time the paraffin solidifies slowly. It can be assumed that the solid–liquid interface location is only a function of time in paraffin storage. This assumption is used when solving the equations. In salt hydrate storage the steel fin does not rapidly achieve the temperature of the wall when compared to the aluminium fin. This is because of its poorer heat conductivity. In salt hydrate storage the solid–liquid interface location is more a function of position and time than a function of time, as has been assumed when solving the equations. This causes an error in the results of the temperature distribution of the fin in salt hydrate storage.

All in all, the best results are achieved when λ is small. The error increases when λ increases. However, the errors made are small, a maximum 0.012 °C for paraffin storage and 0.58 °C in salt hydrate storage in these cases. The mathematical solution for the temperature distribution of the fin works well, especially when paraffin storage with an aluminium fin is concerned.

In Fig. 6a–f, the one-dimensional analytical and numerical results of the solid–liquid interface location in different test cases are shown.

The difference in solid–liquid interface location S_y between one-dimensional analytical and numerical results is relatively small in both paraffin and salt hydrate storage. The biggest error is made in the cases when is large because of the assumption that the location of the solid–liquid interface is only a function of time. In a long fin the location should be a function of time and position. However, the mathematical solution for the solid–liquid interface location performs adequately.

Thus, the assumptions made when solving the equations mathematically do not greatly affect the accuracy of the one-dimensional analytical solution.

5.4. Accuracy of the one-dimensional analytical model

Finally, when the one-dimensional analytical model is compared to the two-dimensional numerical model it is possible to draw conclusions about the accuracy of the analytical model. Fig. 5a–f shows one-dimensional analytical and two-dimensional numerical results of the temperature distribution of the fin in the different test cases.

The results are similar to Section 5.2. The maximum temperature difference (ΔT_{max}) between the one-dimensional analytical results and the two-dimensional numerical results are small when λ is

small, and are largest when λ approaches unity. The analytical model predicts the fin temperature well when the geometry of the cell is close to a one-dimensional case (λ is small or large) and fails to some extent in a pure two-dimensional situation ($\lambda = 1$).

The one-dimensional analytical and two-dimensional numerical results for the solid–liquid interface location are shown in Fig. 6a–f.

When λ is small, the solid–liquid interface in the y-direction moves more slowly in the one-dimensional analytical model than in the two-dimensional model. When λ increases, the location of the solid–liquid interface in a one-dimensional analytical model will go ahead of the interface location in a two-dimensional model. The same conclusions were evident in Section 5.2.

In general, the simplified analytical model more accurately predicts the solid–liquid interface location than the temperature distribution of the fin in the PCM storage with internal fins. The assumptions made when the two-dimensional heat transfer problem was changed to the one-dimensional problem more greatly affect the accuracy of the one-dimensional analytical model than the assumptions made when solving the one-dimensional equations mathematically.

5.5. Fraction of the solidified PCM

The fraction of solidified PCM describes how much of the storage is solidified after a certain time. The factor takes values between 0 (the storage is totally liquid) and 1 (the storage is totally solid). It describes with one value the relative amount of released energy from the storage. Therefore, it is a useful quantity when different methods are compared with each other.

The factor is defined as the volume of the solidified PCM related to the total volume of PCM in the storage:

$$\varepsilon = \frac{2S_x(L_c - D - S_y) + S_y^- L_f}{(L_c - D)L_f} \tag{48}$$

where S_y^- is the average value of the solid–liquid interface location in the y-direction along the fin length and S_x and S_y^- can be calculated from Eqs. (28)–(31).

The rate of solidified PCM calculated from the one-dimensional analytical (Eq. (47)) and two-dimensional numerical results in different test cases are shown in Table 3.

The difference is smaller than ±2.8 % in all cases. If we consider Fig. 6a–f, it can be seen that in many cases the analytical results of the solid–liquid interface location are ahead of the numerical

Table 3
The rate of the solidified PCM calculated with one-dimensional analytical and two-dimensional numerical models in different test cases

Case	$\lambda = L_f/L_c$	Time, s	$T_w - T_m$, °C	D, m	Fraction analytical	Fraction numerical	Error, %
Case 1, para	0.2	724	15	0.0005	0.787	0.799	−1.2
Case 2, para	1	1085	15	0.0005	0.258	0.233	2.4
Case 3, para	5	1085	15	0.0005	0.543	0.539	0.4
Case 4, salt	0.2	169	15	0.0005	0.733	0.749	−1.7
Case 5, salt	1	4226	15	0.0005	0.804	0.826	−2.3
Case 6, salt	5	1127	15	0.0005	0.819	0.791	2.8

results of the interface. At the same time the cross-section of the analytical results in region 1 and region 2 is sharp, though it should be more rounded at the corners. Thus, the numerical results for the solid–liquid interface location are ahead of the analytical results for the interface locations in the corners. The interaction of these errors diminishes the error made when calculating the rate of solidified PCM.

The error is largest in the cases when λ is equal to one, except in case 6. In case 6 the solid–liquid interface (S_y) in the one-dimensional calculation is much further ahead of the interface achieved in the two-dimensional numerical calculation because the heat capacity of the PCM is ignored in the one-dimensional calculation. When λ is large, the value S_y^- is dominant in Eq. (48), therefore the error in calculating S_y in a one-dimensional case affects the rate of solidified PCM.

It seems that the factor Eq. (48) gives a good picture of how much of the storage is solidified without the need to draw a solid–liquid interface figure. It is possible to see from the results that with small λ values, the speed of the solidification is slower in the analytical model than in the two-dimensional numerical model. In reality, when λ is smaller than one, the heat transfers mainly in the x-direction in the storage. In this paper it has been assumed that the heat transfers only in the x-direction and the heat transfer in the y-direction is assumed to be negligible in region 1. Therefore, the location of the solid–liquid interface moves more slowly in analytical results than in numerical results.

When λ increases, the solid–liquid interface calculated by the analytical model starts to move faster than the interface calculated with the two-dimensional analytical model. When λ is over one, the heat transfer is dominant in the y-direction.

In the approximate analytical model in region 2 the sensible heat of the PCM is ignored. Therefore, the analytical method overestimates the actual solid–liquid interface location.

The factor is also useful when dimensioning PCM storage and also when different geometry are compared with each other. With the analytical model it is possible to access how the geometry of the storage and the material properties effect the solidification time of the storage. However, the fraction of solidified PCM is a bulk measure and it misses microscopic effects in the PCM operation. The factor is a useful tool together with analytical results that indicate the location of the solid–liquid interface. For example, Fig. 7 shows the rate of the solidified PCM as a function of time for paraffin storage with the aluminium fin (case 2) and for salt hydrate storage with the steel

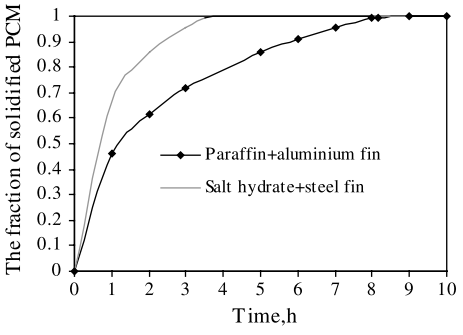

Fig. 7. The fraction of solidified PCM for n-octadecane storage with the aluminium fin and for salt hydrate storage with the steel fin, $T_w - T_m = 15$ °C, $D = 0.0005$ m, $\lambda = L_c/L_f = 0.05/0.05 = 1$.

fin (case 4). The volume of the storage as well as the temperature difference between the wall and the phase change material are the same in both cases.

It can be seen that salt hydrate storage solidifies much more quickly than paraffin storage because of salt hydrates better heat conductivity. The mass of the phase change material in the storages is equal. The storages release different amounts of heat because of different densities and the latent heat of fusion. When the storage volume is in both cases 125 cm^2 (the storage size $0.05 \times 0.05 \times 0.05$ m), the released energy from the paraffin is $E = 25.5$ kJ and from salt hydrate storage $E = 27.1$ kJ during the phase change. In this case the salt hydrate storage works more effectively than the paraffin storage.

6. Conclusions

This paper presents a simplified analytical model based on a quasi-linear, transient, thin-fin equation which predicts the solid–liquid interface location and temperature distribution of the fin in a solidification process with constant end-wall temperatures in a finite PCM storage. The analytical solution consists of the well-known Neumann solution for predicting the solid–liquid interface location S_x in the x-direction, as well as a derived analytical solution to predict the temperature distribution of the fin T_f in the x-direction and the solid–liquid interface location S_y in the y-direction. Some simplifying assumptions are made to make it possible to find an analytical solution to the problem.

A new factor, called the fraction of solidified PCM, is also presented. The factor indicates how much PCM has solidified after a certain time. In addition to the one-dimensional analytical model, the heat transfer in the PCM storage is calculated using the simplified one-dimensional numerical model and the two-dimensional numerical model. Six different test cases were chosen to compare the results by using same initial and boundary values and material properties. The following conclusions are made concerning the accuracy of the one-dimensional analytical model:

- The geometry of the computational domain (cell) seems to be one of the most important factors in explaining the performance of the developed one-dimensional model. When the width to height ratio (λ) is small or large, the accuracy of the one-dimensional approach is relatively good because the heat transfer is near to a one-dimensional model in the x-direction (λ is small) or the y-direction (λ is large). When λ is equal to one, the heat effectively transfers both in the x- and y-direction. By using a one-dimensional approach instead of a two-dimensional approach, the accuracy is slightly reduced. However, the results are still satisfactory, especially for the solid–liquid interface location.
- The assumptions made in order to enable the analytical solution have a minor influence on the results. Thus, the accuracy of the analytical solution is good.
- The assumptions made in simplifying the two-dimensional heat transfer problem into a one-dimensional form affect the accuracy to a greater extent than the assumptions made when solving the one-dimensional equations analytically.
- All in all, the accuracy of the approximate analytical model is good. The model is useful in the pre-design stage of the storage. With the model it is possible to compare several storage alternatives in a reasonable time.

Acknowledgements

The support of The Academy of Finland and the Graduate School of Building Physics at HUT are greatly acknowledged by the authors.

References

[1] P.V. Padmanabhan, M.V. Murthy, Outward phase change in a cylindrical annulus with axial fins on the inner tube, International Journal of Heat and Mass Transfer 29 (12) (1986) 1855–1868.
[2] R. Velraj et al., Heat transfer enhancement in a latent heat storage system, Solar Energy 65 (3) (1999) 171–180.
[3] P.G. Kroeger, S. Ostrach, The solution of a two-dimensional freezing problem including convection effects in the liquid region, International Journal of Heat and Mass Transfer 17 (1973) 1191–1207.
[4] G. Lane, in: Solar Heat Storage: Latent Heat Material, vol. 1, CRC Press, 1983.
[5] www.frisby.com.
[6] R. Siegel, Solidification of low conductivity material containing dispersed high conductivity particles, International Journal of Heat and Mass Transfer 22 (1977) 1087–1089.
[7] H. Mehling, S. Hiebler, F. Ziegler, Latent heat storage using a PCM-graphite composite material, in: Terrastock 8th International Conference on Thermal Energy Storage, 28 August–1 September, 2000, Proceedings, vol. 1, 2000, pp. 375–380.
[8] R. Velraj, R. Seeniraj, B. Hafner, et al., Experimental analysis and numerical modelling of inward solidification on a finned vertical tube for a latent heat storage unit, Solar Energy 60 (5) (1997) 281–290.
[9] S. Al-Jandal, Experimental study of temperature dependent heat transfer during melting and solidification processes, in: 2nd World Renewable Energy Congress, Reading University, UK, 13–18 September 1992, pp. 1097–1105.
[10] I. Bujage, Enhancing thermal response of latent heat storage systems, International Journal of Energy Research 21 (1997) 759–766.
[11] U. Stritih, P. Novak, Heat transfer enhancement at phase change processes, in: Terrastock 8th International Conference on Thermal Energy Storage, 28 August–1 September, 2000, Proceedings, vol. 1, 2000, pp. 333–338.
[12] W. Humphries, E. Griggs, A design handbook for phase change thermal control and energy storage devices, NASA TP-1074, 1977.
[13] P. Lamberg, K. Sirén, Analytical model for melting in semi-infinite PCM storage with an internal fin, Heat and Mass Transfer 39 (2003) 167–176.
[14] www.femlab.com.
[15] V. Alexiades, A.D. Solomon, Mathematical Modelling of Melting and Freezing Processes, Hemisphere Publishing Corporation, USA, 1993.
[16] R. Henze, J. Humphrey, Enhanced heat conduction in phase-change thermal energy storage devices, International Journal of Heat and Mass Transfer 24 (1981) 450–474.
[17] H. Carslaw, J. Jaeger, Conduction of Heat in solids, second ed., Oxford University Press, New York, 1959.
[18] K.A. Rathjen, M.J. Latif, Heat conduction with melting or freezing in a corner, Journal of Heat Transfer (1971) 101–109.
[19] B. Zivkivic, I. Fujii, An analysis of isothermal phase change of phase change material within rectangular cylindrical containers, Solar Energy 70 (1) (2001) 51–61.
[20] www.climator.com.
[21] F.P. Incropera, D. De Witt, Fundamentals of Heat and Mass Transfer, John Wiley & Sons Inc., Canada, 1990.